Spectrophotometric evaluation of optical performances of polarizing technologies for smart window applications

2014 J. Phys.: Conf. Ser. 547 012013

(http://iopscience.iop.org/1742-6596/547/1/012013)

Journal of Physics: Conference Series **547** (2014) 012013 doi:10.1088/1742-6596/547/1/012013

Spectrophotometric evaluation of optical performances of polarizing technologies for smart window applications

N. Levati, L. Vitali, D. Fustinoni and A. Niro

Politecnico di Milano, Department of Energy,
Campus Bovisa, Via Lambruschini 4, 20156 Milano, Italy

E-mail: alfonso.niro@polimi.it

Abstract. In recent years, window-integrated solar protection systems are used and studied as a promising energy saving technology, both for cold and hot climates. In particular, smart windows, whose optical proprieties in the solar wavelength range can somehow be controlled, show interesting results, especially in reducing the air conditioning power consumption. With the improvement of nanolithography techniques as well as with the possibility of designing polarization intervals, coupled polarizing films show a good potential as a dynamic and wavelength-selective shading technology. In this paper, UV-Vis-NIR spectrophotometric measurements are carried out on two polarizing technologies, Polaroid crystalline polarizer and Wire Grid broadband polarizer, in single- and double- film layout, to evaluate their optical performances, i.e. spectral transmittance, reflectance and absorptivity. The solar radiation glazing factors, according to the standard UNI EN 410, are calculated. The measured data are also analyzed in detail to emphasize the optical peculiarities of the materials under study that do not stand out from the standard parameters, as well as the specific problems that arise in spectrophotometric evaluations of polarizing films.

1. Introduction

Through the history of thermal and lightning control for human comfort in indoor spaces, transparent windows have been coupled with a large variety of shading solutions. Since 1959, with the invention of the float (Pilkington) method, that allowed industrial production of glasses with uniform thickness and very flat and parallel surfaces, and in the following years thanks to the advancements in metallic and polymeric materials engineering, many research projects have been carried out on window-integrated solar protection systems.

Today, three main types of such systems can be identified. *Static/Passive* glasses have fixed optical properties, i.e. spectral transmittance, reflectance and absorptivity, determined by the use of purposely engineered superficial thin films or by multiple layer deposition. This category includes various kinds of low-emissivity (Low-E) glasses and selective coatings (solar control glasses). *Dynamic/Passive* glasses show a change in optical proprieties due to incoming solar radiation, like thermocromic (TC) and photocromatic (PC) glasses, while *Dynamic/Active* glasses require an external electric stimulus, that usually allows a greater flexibility of use and the optimization of daylighting and energy saving. Examples are Electrocromic (EC), Liquid Crystal glasses (LCD) and Suspended Particle Devices (SPD).

In recent years, researchers, standardization bodies, governement bodies and industrial companies are closely following the development and performance improvement of the aforementioned technologies. Among recent publications, the paper by Jelle [1] reports a comprehensive comparison of thermo-optical performances of several smart windows technologies, as well as a deep reference section. The report by Lee et al. [2] focuses on an experimental and numerical evaluation of the reduction of Heating, Ventilation and Air Conditioning (HVAC) power consumption given by the use of TC and EC smart windows in a test building, showing promising results in the case of EC windows, also studied by Sbar [3]. A previous study on the control strategy for active windows was carried out by Jonsson and Roos [4]. In Italy, spectrophotometric measurements were performed by Asdrubali et al. [5] on glass and plastic based window panes.

Fewer literature can be found on polarizing filters as a possible technology for a new concept of smart windows, that can combine the benefits of a passive approach (no energy is required to maintain a certain optical configuration) with the reconfiguration capability of active technologies. The recent development of nanolitographic techniques can lead to the design of the polarization spectral range, and to special films suited for both applications and climate zones.

In this paper, UV-Vis-NIR spectrophotometric measurements are carried out to measure the global optical performances, i.e., transmittance, reflectance and absorptivity parameters according to the standard UNI EN 410 [6], of two polarizing technologies, namely crystalline polarizer and Wire Grid broadband polarizer, in single- and double- film layout. The measured data are analyzed in detail to emphasize the optical peculiarities of the materials under study that do not stand out from the standard parameters, and to evaluate any issues that can arise in spectrophotometric measurements of polarizer filters.

2. Experiments

2.1. Theory and definitions

Let us consider an ideal linearly polarized beam, whose each wavelength component is totally polarized, with total intensity I_0, incident on an ideal polarizer filter; the total intensity of the transmitted radiation I is, according to Malus' law (1):

$$I = I_0 \cos^2 \varphi_l \tag{1}$$

where φ_l is the angle between the initial polarization orientation of the beam and the polarizer axis. When a beam of unpolarized radiation, like sunlight, is transmitted by a single polarizing film, its intensity is reduced by the average of $\cos^2(\varphi)$ within the 0-π interval, i.e., by one half. Thus, Malus' law applied in the case of two ideal polarizing filters crossed by unpolarized radiation can be written as (2):

$$I = \frac{1}{2} I_0 \cos^2 \varphi \tag{2}$$

where φ is the angle between the axis of the two polarizers. While being applicable to limited ranges and for certain polarizing technologies, this physical principle is not adequate to predict the behaviour of wavelength-selective polarizers, that must be experimentally evaluated.

On the other hand, the standard UNI EN 410 defines some global parameters to evaluate the performances of luminous and solar characteristics of glazing for glass in buildings. Light (visible) transmittance τ_v and reflectance ρ_v are defined by equations (3-4)

$$\tau_v = \frac{\sum_{\lambda=380\,nm}^{780\,nm} D_\lambda \tau(\lambda) V(\lambda)\,\Delta\lambda}{\sum_{\lambda=380\,nm}^{780\,nm} D_\lambda V(\lambda)\,\Delta\lambda} \tag{3}$$

$$\rho_v = \frac{\sum_{\lambda=380\,nm}^{780\,nm} D_\lambda \rho(\lambda) V(\lambda)\,\Delta\lambda}{\sum_{\lambda=380\,nm}^{780\,nm} D_\lambda V(\lambda)\,\Delta\lambda} \tag{4}$$

where D_λ is the relative spectral distribution of illuminant D65 and V(λ) is the spectral luminous efficiency for photopic vision defining the standard observer for photometry or, in other words, the sensibility curve of an average human eye (figure 1).

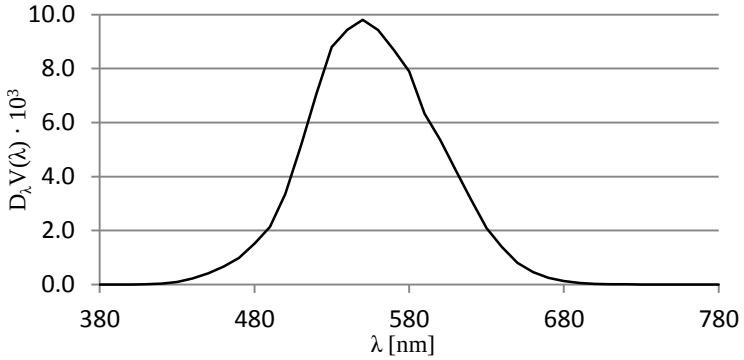

Figure 1. Visible parameters weight factor vs. wavelength

Solar direct transmittance τ_e and reflectance ρ_e are defined by equations (5-6)

$$\tau_e = \frac{\sum_{\lambda=300\,nm}^{2500\,nm} S_\lambda \tau(\lambda)\,\Delta\lambda}{\sum_{\lambda=300\,nm}^{2500\,nm} S_\lambda\,\Delta\lambda} \tag{5}$$

$$\rho_e = \frac{\sum_{\lambda=300\,nm}^{2500\,nm} S_\lambda \rho(\lambda)\,\Delta\lambda}{\sum_{\lambda=300\,nm}^{2500\,nm} S_\lambda\,\Delta\lambda} \tag{6}$$

where S_λ is the relative spectral distribution of the solar radiation (figure 2)

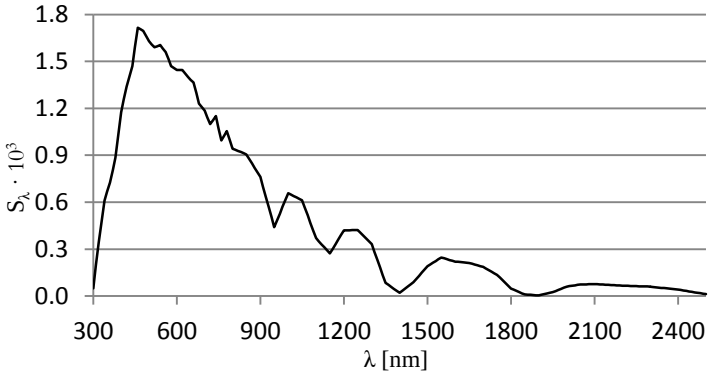

Figure 2. Solar parameters weight factor vs. wavelength

UV transmittance is defined by equation (7). Although the UV range is conventionally limited between 280 and 315 nm for the UV-B band, and from 315 to 380 nm for the UV-A band, our analysis starts at 300 nm, since shorter wavelengths do not reach ground level because of atmospheric absorption [7].

$$\tau_{uv} = \frac{\sum_{\lambda=280\,nm}^{380\,nm} U_\lambda \tau(\lambda)\,\Delta\lambda}{\sum_{\lambda=280\,nm}^{380\,nm} U_\lambda\,\Delta\lambda} \tag{7}$$

These parameters are directly calculated from spectral transmittance τ(λ) and reflectance ρ(λ) measurements. Visible and solar absorptivity, i.e., α_v and $\alpha_{e,}$ are instead derived from the relation between the three radiative proprieties, both spectral and total, equations (8-9).

$$\alpha(\lambda) = 1 - (\tau(\lambda) + \rho(\lambda)) \tag{8}$$

$$\alpha_e = 1 - (\tau_e + \rho_e) \tag{9}$$

2.2. Experimental setup

Two different polarizing materials are analyzed, in single-film (polarizer only) and double-film (polarizer/analyzer) configurations. One is a Polaroid polymeric-crystalline filter: each film is 0.13 mm thick and it is composed by an inner layer of polyvinyl-alcohol (PVA) with uniformly oriented iodoquinine sulphate crystals, laminated between two external layers of triacetate-cellulose (TAC). The other is a wire grid (WG) anisotropic polarizer, whose polarizing element is a layer of 100 nm-high aluminium nanowires deposited on a TAC substrate with a pitch of 100 nm, as schematically shown in figure 3, for a total film thickness of 0.08 mm.

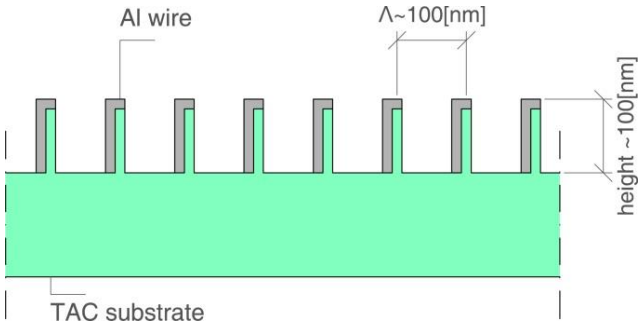

Figure 3. Scheme of the wire grid polarizer film

The samples, measuring 45 mm x 45 mm, are glued on an octagonal wood frame with a central aperture, as shown in figures 4 and 5. Henceforth, φ is the angle between the axis of the two polarizers, θ is the angle of the sample orientation with respect to the vertical, for both single- and double-film trial configurations.

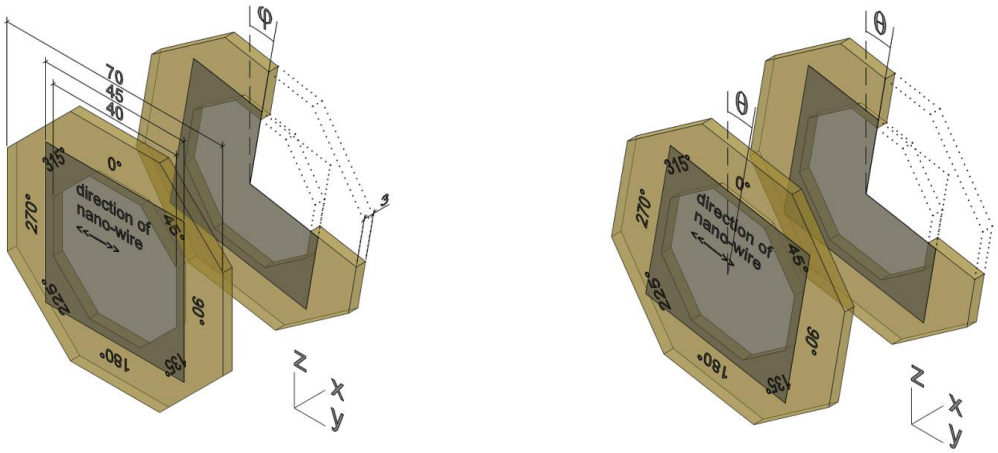

(a) (b)

Figure 4. 3D drawing of the frame-mounted WG samples.

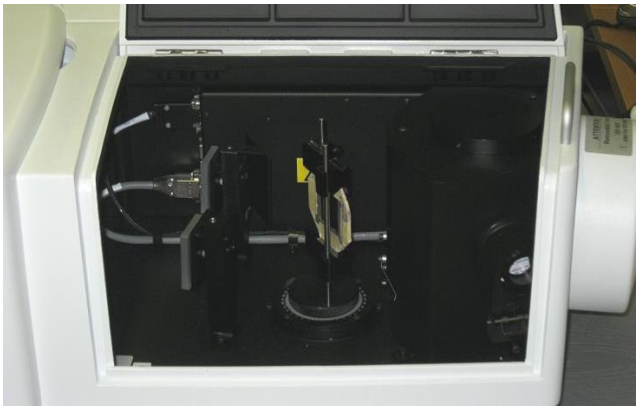

Figure 5. Photo of the sample (center) and integrating sphere (right) in the integrating sphere accessory.

The instrument used in this work is a Perkin Elmer Lambda 950 UV-Vis-NIR, double beam, double monochromator spectrophotometer. The radiation sources are a deuterium lamp for the UV region, and a tungsten lamp for the Vis/NIR range. The instrument is equipped with a 150 mm spectralon integrating sphere mounting a Photomultiplier Tube (PMT) sensor for the UV-Vis range, and a Gallium Arsenide (InGaAs) sensor for NIR measurements; the switch between the two detectors occurs at 860 nm. The total spectral range is between 200 and 2500 nm with a wavelength accuracy of ±0.08 nm in the UV/Vis range, and ±0.30 nm in the NIR range. The instrument have been calibrated with a certified Spectralon sample; the measurement errors, both in reflectance and transmittance mode, are less than 0.11% in the UV-Vis range, and less than 0.23% in the NIR range. In this work, the measurement range is between 300 and 2500 nm with 10 nm intervals. A Hanle-type common beam depolarizer, placed behind the ray chopper, minimizes the unwanted polarization of both test and reference beams caused by the instrument optics [8], even though some residual polarization effects are still noticeable in sections *3.1.1* and *3.2.1*.

The optical scheme of the integrating sphere is shown in figure 6. For transmittance measurements, the sample is placed in a rotating sample holder shown in figure 5, while for reflectance measurements the sample is placed in the reflectance sample holder located in the backside of the sphere, with a fixed 8° inclination relative to the incoming beam (quasi-parallel). It's worth remembering that reflectance measurements encompass both specular and diffuse components.

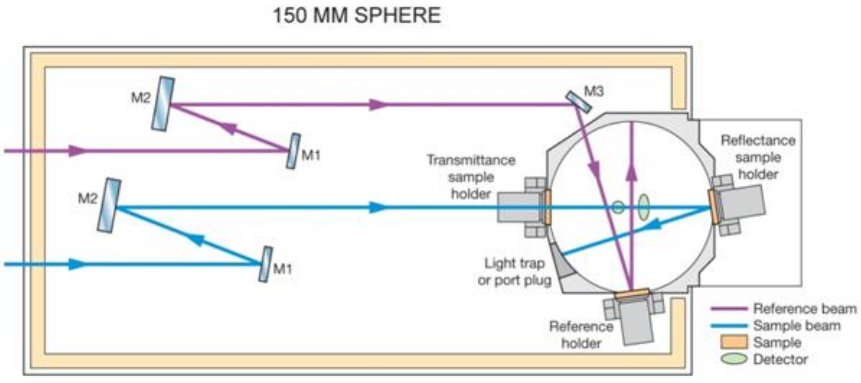

Figure 6. Optical scheme of the Integrating Sphere accessory (adapted from [9])

Data are collected with a PC using a Perkin Elmer dedicated software (UV Winlab) and analyzed with a custom made datasheet.

2.3. Preliminary analysis: scattering effects

As stated in EN 410, "the use of an integrating sphere is necessary when light scattering materials are tested", and "the size of the sphere and its aperture shall be large enough to collect all possible scattered light". In order to test the adequacy of the employed integrating sphere, the WG single-film specimen spectral transmittance has been measured by placing the specimen both close to the aperture and in the rotating sample holder, mounted 6 cm apart. As shown in figure 7, the two measurements differ at the most of 0,3% in the UV-Vis range, and of 1% in the NIR region; thus, for our purposes, scattering phenomena can be neglected.

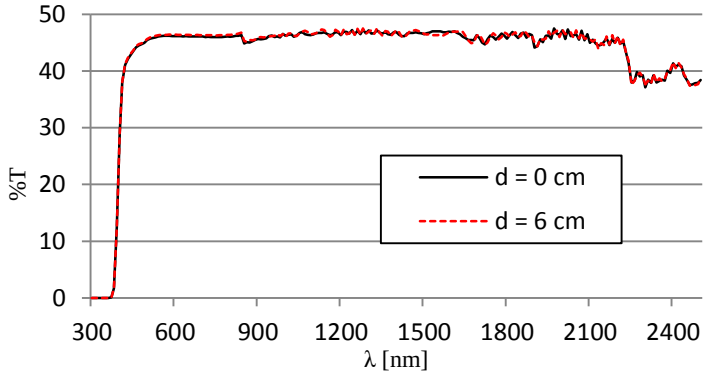

Figure 7. Single WG film, placed at the entrance of the integrating sphere (d = 0 cm) and on the rotating sample holder (d = 6 cm)

3. Results

3.1. Crystalline polarizer (Polaroid)

3.1.1. Single film. A single film of Polaroid has been preliminary tested in four orientations, namely θ = 0°, 45°, 90°, 135°. As shown in figure 8, only the visible part of the spectrum shows a partial agreement to Malus' law (equation 2); in fact, UV radiation is completely blocked, while the specimen is 90% transparent in most of the NIR region, amd hence only the visible portion of the spectrum is effectively polarized. Transmittance values show a little difference with the orientation, about 3%, again only in the visible range, between 0°/45° and 90°/135°, probably because of residual beam polarization combined with the polarized light dependence on the PMT sensor [10].

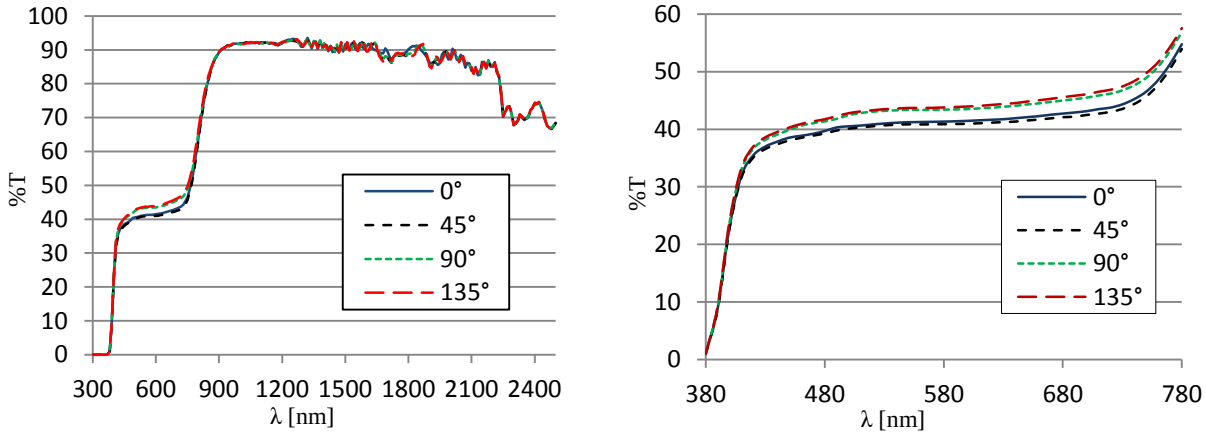

(a) (b)

Figure 8. $\tau(\lambda)$, single Polaroid film, various orientations θ: full spectrum (a) and Vis range detail (b)

To reduce this effect, the subsequent transmittance and reflectance measurements on the coupled films are averaged on four orientations, as in equation (11), also applicable to $\rho(\lambda)$.

$$\tau(\lambda) = \bar{\tau}(\lambda) = \frac{\sum_{i=1}^{4} \tau_{\theta_i}(\lambda)}{4} \quad \text{for } \theta_i = 0°, 45°, 90°, 135° \tag{11}$$

3.1.2. Double film, clear configuration (φ=0°). The total optical proprieties of the double-film specimen have been tested. Compared to the single film, $\tau(\lambda)$ is reduced almost uniformly by 6-10%, whereas $\rho(\lambda)$ is almost constant around 10%. The calculated absorptivity, $\alpha(\lambda)$, shows clearly the filter behavior; since reflectance is uniformely low, UV radiation is almost totally absorbed, just like the non-transmitted part of visible radiation (figure 9).

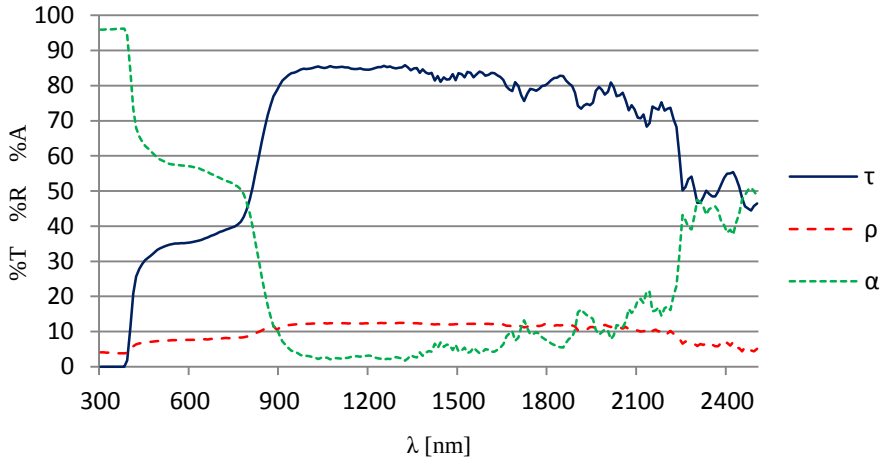

Figure 9. Transmittance, reflectance and absorptivity vs. wavelength for a double Polaroid film, φ = 0°

3.1.3. Double film, variable configuration. This test shows, as graphed in figure 10, the good agreement with Malus' theory for the Polaroid filters in the Vis region; $\tau(\lambda)$ is reduced by half for φ = 45°, and completely blocked for φ = 90°. The UV and NIR behavior remains almost unchanged, as well as spectral reflectance (not shown); in particular, even in the dark configuration, the filter is almost transparent within most of the NIR range.

.

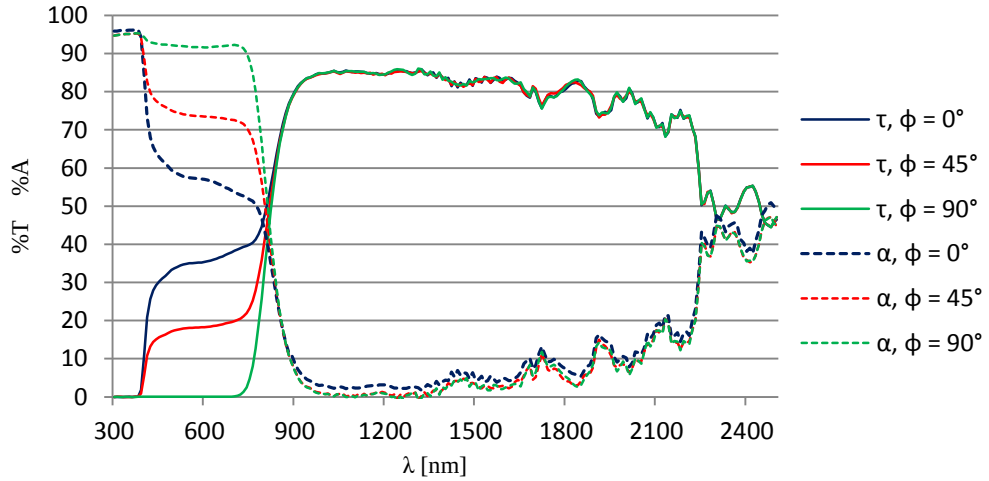

Figure 10. Transmittance and absorptivity vs. wavelength for a double Polaroid film, various φ

3.2. Wire Grid polarizer

3.2.1. *Single film.* Just like the Polaroid film, the single WG film shows little differences in the Vis region for $\tau(\lambda)$, while varying its orientation θ. In particular, artifacts of 1.5% for $\theta = 45°$ and 1.7% for $\theta = 135°$ are visible in Figure 11 at 860 nm, where detector is swiched, due to polarized light dependence of PMT readings [11]. Transmittance values are almost constant and just below 50%, and this is a hint of the main feature of the WG film, that is the ability to polarize NIR radiation. UV radiation is totally blocked, but in a different way with respect to the Polaroid filter; i.e. radiation is absorbed and reflected in equal parts, whereas it is completely absorbed by the Polaroid filter.

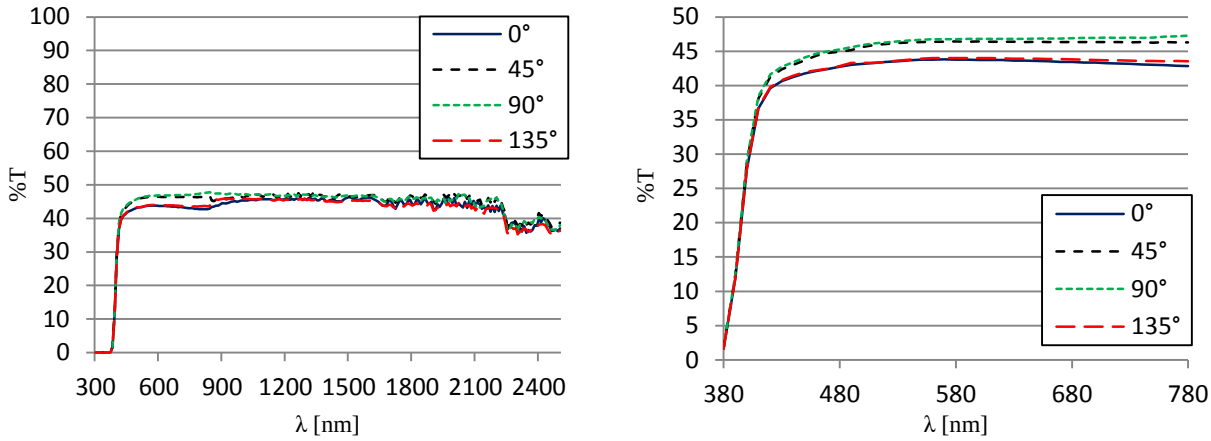

Figure 11. $\tau(\lambda)$, single WG film, various orientations θ: full spectrum (a) and Vis range detail (b)

3.2.2. Double film, clear configuration (φ=0°). The double-film specimen shows, in the $\varphi = 0°$ (clear) configuration, a slight and almost uniform transmittance reduction of 5% as compared with the single film. As showed in figure 12, reflectance is around 50% in the whole range, while absorptivity values show different behaviors from UV (50%), to Vis (15%) and to NIR (5% from 850 nm to 2200 nm, 20% to 2500 nm).

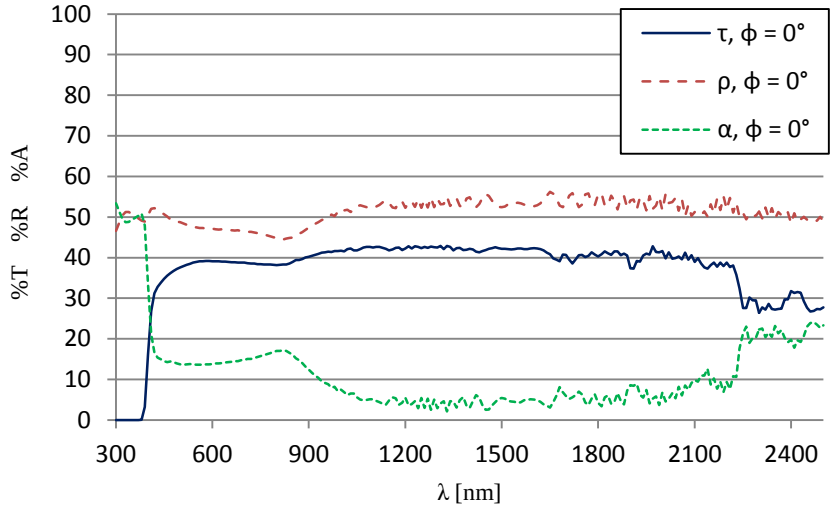

Figure 12. Transmittance, reflectance and absorptivity vs. wavelength for a double WG film, $\varphi = 0°$

3.2.3. Double film, variable configuration. Varying the rotation angle φ shows some interesting behaviors, namely, the NIR radiation polarization effect, the non-linearity between φ and the transmittance attenuation (or reflectance enhancement), mainly caused by inter-reflections, the independence of UV behavior from φ, and the total radiation blockage for $\varphi = 90°$. Moreover, the local reflectance minimum around 800 nm, typical of aluminum, is enhanced by closing the filter, as it can be seen in figure 13(b).

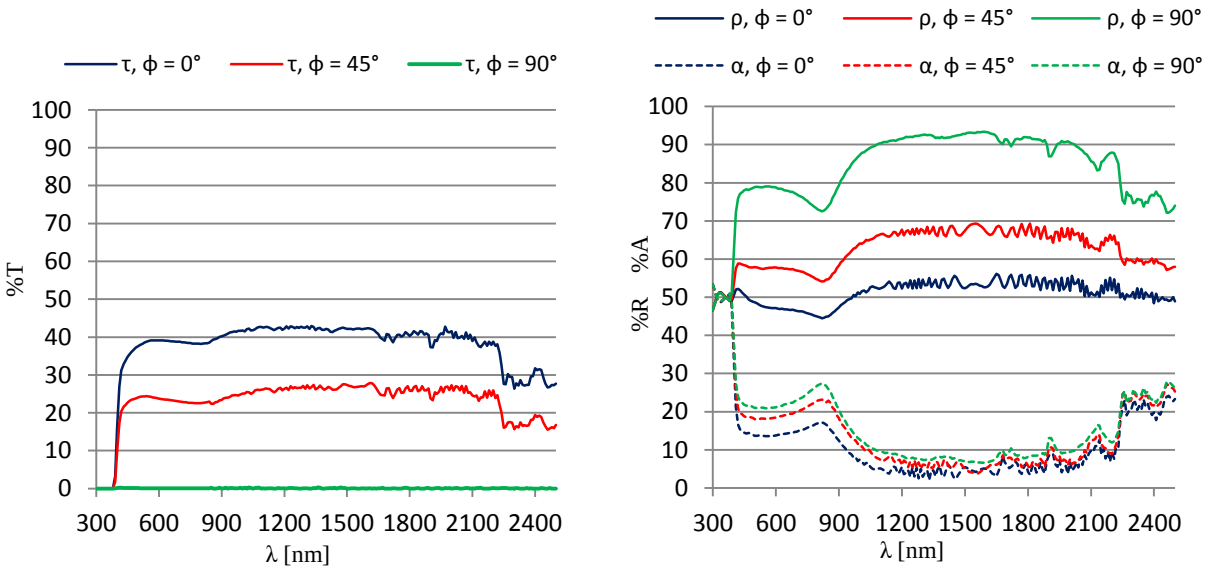

(a) (b)

Figure 13. Transmittance (a), reflectance and absorptivity (b) vs. wavelength for a double WG film, various φ

3.3. Global parameters

The calculated global solar radiation glazing factors are reported in table 1. Clear ($\varphi = 0°$), gray ($\varphi = 45°$) and dark ($\varphi = 90°$) configurations are considered for visible and solar transmittance parameters, clear and dark for UV transmittance, visible and solar transmittance, and solar absorption. These parameters summarize what can be seen in figures 8-13, i.e., UV radiation is completely blocked by both Polaroid and WG samples, while the WG specimen shows a better overall visible transmission and the capability of NIR transmission control.

Table 1. Calculated solar radiation glazing factors

	τ_{uv}	τ_{uv}	τ_v			ρ_v		τ_e			ρ_e		α_e	
φ[°]	0	90	0	45	90	0	90	0	45	90	0	90	0	90
P_1	0.1	-	44.0	-	-	6.6		57.6	-	-	6.9	-	35.5	-
WG_1	0.1	-	47.0	-	-	46.0	-	42.3	-	-	45.9	-	11.9	-
P_2	0.0	0.0	36.1	18.3	0.0	7.5	8.2	49.4	40.3	30.7	8.8	9.7	41.8	59.6
WG_2	0.0	0.0	40.6	24.5	0.1	46.8	85.2	36.7	22.4	0.1	47.0	78.9	16.2	21.0

P and WG Subscripts indicate the number of films

4. Conclusions

The Polaroid crystalline polarizer shows excellent UV blocking proprieties and a good agreement in the Vis range with Malus theory, so that it can be used as a test reference. However, the poor Vis transmittance in the double film clear state ($\tau_{v,\,\varphi=0°} = 36.1$), and the high NIR transmittance, as well, in

every configuration do not allow its use for effective smart windows. Wire Grid polarizer shows a much more interesting behavior, due to the ability of polarizing NIR radiation, as well as to both low solar absorption ($\alpha_{e\ ,\ \varphi = 90°} = 21.0$) and high reflectance ($\rho_{e\ ,\ \varphi = 90°} = 78.9$) especially in the dark state. In particular, low values of α_e are required in hot climates to avoid the thermal shocks in glasses. More advances are expected with the diffusion of nanolitographic techniques that will allow, at a certain degree, the control over the spectral characteristics of Wire Grid filters.
The measurements have been made using the UNI EN 410 as reference, but the norm needs to be improved to take into account this kind of materials and, in general, smart glasses. In particular, polarization effects must be taken into account for more reliable spectrophotometric measurements, especially in the visible wavelength range. Further work is needed on the spectral characterization of polarizing technologies, especially in layered glass-integrated configurations, and with variable angle of incidence.

References

[1] Jelle B P 2013 *Solar En. Mat. & Solar cells* **116** 291-323
[2] Lee E S, Fernandes L L, Goudey C H, Jonsson C J, Curcija D C, Pang X, DiBartolomeo D and Hoffmann S 2013 A Pilot Demonstration of Electrochromic and Thermochromic Windows in the Denver Federal Center, Building 41, Denver, Colorado *U.S. General Services Administration report* available online
[3] Sbar N L, Podbelski L, Yang H M and Pease B 2012 *Int. J. of Sust. Built Env.***1** 125-39
[4] Jonsson A and Roos A 2010 *Sol. En.* **84** 1-9
[5] Asdrubali F, Buratti C and Baldinelli G 2000 Misure spettrofotometriche su materiali trasparenti per chiusure perimetrali in edilizia *55th Congresso Nazionale ATI (Bari-Matera)*
[6] UNI EN 410:2011 Glass in Building – determination of luminous and solar characteristics of glazing
[7] Rottman G 2006 *Space Sci. Rev.* **125** 39-51
[8] Taylor J L 2009 Eliminating the inherent polarization artifact of UV/Vis/NIR spectrophotometers *Perkin Elmer UV/Vis/NIR spectroscopy resource page* online at http://pe.taylorjl.net/PE_Blog/
[9] 2009 Transmission measurements using integrating spheres for the Lambda 950/850/650 UV/Vis/NIR and UV/Vis spectrophotometers *Perkin Elmer application note* available online
[10] Hamamatsu Photonics K. K. Editorial Committee 2007 *Photomultiplier tubes – basics and applications* Word Technical Writing, Inc. (Hamamatsu Photonics K. K. Electron Tube Division) chapter 4 pp 78–80 available online
[11] Taylor J L 2009 The grating/detector change in a UV/Vis/NIR instrument: polarization in specular reflectance measurements *Perkin Elmer UV/Vis/NIR spectroscopy resource page* online at http://pe.taylorjl.net/PE_Blog/